The Armed Forces Institute of Pathology
Department of Veterinary Pathology

Conference Coordinator:
Todd M. Bell, DVM

WEDNESDAY SLIDE CONFERENCE 2008-2009

Conference 6

22 October 2008

Conference Moderator:

Dr. Lauren Brinster, DVM, Diplomate ACVP

CASE I – Case DG0802868 (AFIP 3106794)

Signalment: 2-year-old male beagle dog

History: This animal was part of an IACUC approved animal study to evaluate the pathogenesis and treatment of septic shock. The dog had been anesthetized and an intrabronchial inoculation of *Staphylococcus aureus* was placed into the right caudal lobe. The dog was sedated with fentanyl, versed and medetomidine and was mechanically ventilated via an endotracheally tube for 89 hours. Intravenous fluid administration with Normosol was provided to maintain blood pressure and hydration. Oxygen was administered to maintain adequate arterial oxygenation. After 24 hours reduced arterial oxygenation required the level of oxygen administration to be increased to 100%. The dog died after 89 hours, seven hours before the termination point for the study. The post-mortem interval was 10 hours at refrigeration temperature.

Gross Pathology: At necropsy this animal was well muscled with a moderate amount of body fat and in good hydration. Edema was noted in the subcutaneous tissues of the ventral neck and thorax. Approximately 500 ml of clear serosanguineous fluid was present in the abdominal cavity and approximately 400 ml of similar fluid was present in the thoracic cavity. The lungs were moderately atelectatic secondary to the presence of the pleural effusion. An area within the right caudal lobe measuring approximately 3 cm x 3 cm was noted to be pale with demarcated borders consistent with a focus of necrosis, which corresponded to the placement of the bacterial clot. All lung lobes were firm and sank in formalin. Multifocal petechial and ecchymotic hemorrhages were noted in the pancreas and mesentery. The liver, kidneys and spleen were moderately congested. The remaining organs and tissues appeared normal.

Laboratory Results: Samples for bacterial culture were collected from the femoral and jugular catheters, which yielded a mixed growth of Klebsiella pneumonia and *Acinetobacter baumannii*.

Histopathologic Description: There was a severe fibrinosuppurative bronchopneumonia. Bronchioles and alveoli contained large numbers of neutrophils admixed with moderate numbers of alveolar macrophages and fibrin. The bronchi, bronchioles and alveoli were prominently lined by homogeneous eosinophilic granular to fibrillar hyaline membranes **(Fig. 1-1)**. Degenerative cells could be identified within the hyaline membranes in areas. Respiratory epithelium was not evident lining the bronchioles.

***Sponsored by the American Veterinary Medical Association, the American College of Veterinary Pathologists, and the C. L. Davis Foundation.**

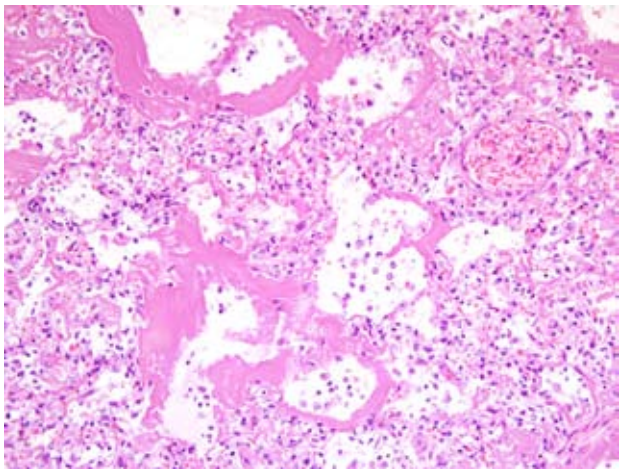

1-1 Lung, dog. Loss of bronchiole and alveolar epithelium with replacement by variably thick, acellular, fibrillar, eosinophilic material (hyaline membranes). (HE 200X).

Contributor's Morphologic Diagnosis:

1. Lung: bronchopneumonia, fibrinosuppurative, severe
2. Lung: hyaline membranes, bronchiolar and alveolar, diffuse
3. Multiple organs: bacteremia, bacterial rods

Contributor's Comment: The suppurative bronchopneumonia associated with intrabronchial administration of Staphylococcus aureus in this case was similar to other dogs examined on this protocol. The atypical feature of the histologic appearance of the bronchopneumonia in this case was the presence of prominent bronchiolar and alveolar hyaline membranes. Hyaline membranes may occur in a variety of disease entities where there is diffuse alveolar damage. In premature infants there is a condition termed hyaline membrane disease of the newborn or respiratory distress syndrome. Hyaline membranes are also a common feature of the Acute Respiratory Distress Syndrome (ARDS). Hyaline membranes are comprised of homogenous granular or fibrillar eosinophilic material, which line alveoli and bronchioles. They are composed of necrotic epithelial cell debris admixed with fibrin and plasma elements.[9] Immunohistochemistry studies in human tissues have demonstrated that the epithelial and endothelial components of surfactant apoprotein A, factor VIII related antigen and cytokeratin AE1/AE3 are present in hyaline membranes associated with diffuse alveolar damage.[8]

Respiratory distress syndrome in premature infants is associated with inadequate levels of pulmonary surfactant produced by type II pneumocytes.[5] Decreased levels of surfactant causes increased alveolar surface tension, which leads to atelectasis, hypoxemia and acidosis. This further causes pulmonary vasoconstriction and hypoperfusion leading to capillary endothelial damage, plasma leakage, fibrin deposition and hyaline membrane formation.

Acute respiratory distress syndrome occurs in a variety of mammalian species including man. ARDS can be due to a variety of etiologic factors such as septic shock, physiologic shock associated with trauma or burns, severe pulmonary viral infections such as SARS, inhaled toxins or irritants such as smoke, phosgene and mercury vapor, hypersensitivity to certain organic solvents and herbicides such as kerosene and paraquat, high altitude, cytotoxic drugs such as bleomycin, busulfan and methotrexate, and oxygen toxicity.[1]The common pathogenesis in these entities is the development of acute diffuse alveolar damage to the alveolar epithelium and capillary endothelium with interstitial and intraalveolar edema and fibrin exudation and the development of hyaline membranes.[6] As a response to the alveolar injury, type II epithelial cells will proliferate and resolution will either lead to recovery or given the severity of the injury may lead to pulmonary fibrosis.

In this case there were multiple interrelated contributing factors, which may have led to the development of pulmonary hyaline membranes, including septic shock, terminal gram negative sepsis, mechanical ventilation injury and oxygen toxicity. The most likely significant cause was oxygen toxicity. Oxygen toxicity has been induced and has been reported to occur in a wide variety of mammalian species. Exposure to oxygen levels of 85-100% for a prolonged period can cause oxygen toxicity. Dogs exposed to 1 atm of oxygen had an average survival time of approximately 60-80 hours.[3] Oxygen derived free radicals including superoxide, hydroxyl ion and singlet oxygen can directly injure cell membrane by causing lipid peroxidation. Additionally, there is inhibition of nucleic acid and protein synthesis and inactivation of cellular enzymes. Damage to pulmonary epithelium may also lead to decreased levels of surfactant. Oxygen toxicity can also induce CNS signs of vertigo and convulsions.[7] Ultrastructurally, studies have shown that as little as 1 to 4 hours of exposure to 100% oxygen can cause morphologic changes to type I epithelial cells with bleb formation of the cytoplasmic membranes and swelling of endothelial cells with plasma transudation.[4]

AFIP Diagnosis:

Lung: Pneumonia,broncho-interstitial, fibrinosuppurative, acute, diffuse, severe with bronchiolar and alveolar hyaline membranes and bacteria

Conference Comment: The contributor gave an excellent explanation of both the cause and pathogenesis of ARDS. Grossly, lungs with this type of insult contain lesions with greater involvement of the dorsocaudal lung fields. Despite the nature of the causative agent, diffuse alveolar damage leads to a predictable histologic pattern of progression from an acute exudative phase to a subacute proliferative phase followed by a chronic fibrosing phase.[2]

Contributing Institution: National Institutes of Health, Division of Veterinary Resources, Bethesda, MD 20892-5280

References:

1. Blennerhassett JB. Shock lung and diffuse alveolar damage pathological and pathogenetic considerations. Pathology **17(2)**:239-47, 1985
2. Caswell JL, Williams KJ: Respiratory system. *In:* Jubb, Kennedy and Palmer's Pathology of Domestic Animals, ed. Maxie MG, 5th ed., vol 2, pp.564-567. Elsevier Limited, Edinburgh, UK, 2007
3. Clark JM, Lambertsen CJ: Pulmonary oxygen toxicity: a review. Pharmacol Rev **23(2)**:37-133, 1971
4. Coalson JJ, Beller JJ, Greenfield LJ: Effects of 100 per cent oxygen ventilation on pulmonary ultrastructure and mechanics. J Pathol **104(4)**:267-73, 1971
5. Hallman M, Glumoff V, Ramet M: Surfactant in respiratory distress syndrome and lung injury. Comp Biochem Physiol A Mol Integr Physiol **129(1)**:287-94, 2001
6. Hasleton PS, Roberts TE: Adult respiratory distress syndrome- an update. Histopathology **34(4)**:285-94, 1999
7. Patel DN, Goel A,, Agarwal SB, Garg P, Lakhani KK: Oxygen toxicity. J Indian Academy of Internal Medicine **4(3)**:234-7, 2003
8. Peres SA, Parra ER, Eher E, Capelozzi VL: Nonhomogenous immunostaining of hyaline membranes in different manifestations of diffuse alveolar damage. Clinics **61(6)**:497-502, 2006
9. Scarpelli EM: Respiratory distress syndrome of the newborn. Annu Rev Med **19**:153-166,1968

II – Case MK 0803123 (AFIP 3106804)

Signalment: 6-year-old male, Rhesus Macaque, (*Macaca mulatta*)

History: An encapsulated subcutaneous mass was noted near the right nipple. It was removed and submitted for analysis. On physical exam no other abnormalities were noted.

Gross Pathology: The tissue sample (biopsy) measured 1.8 x 1.5 x 1.0 cm. The mass is firm, slightly nodular and yellow to white in color. It is encapsulated in a well demarcated capsule.

Laboratory Results: None performed.

Histopathologic Description: The slide consists of a well demarcated neoplasm surrounded by a layer of smooth muscle lined by flattened epithelial cell. There are some pockets of normal glandular tissue in the surrounding soft tissue. The neoplastic nodules appear to be mostly solid with rare ductal and tubular structures. The ductal structures are lined by pleomorphic epithelial cells with loss of polarity and piling up of cells **(Figs. 2-1, 2-2)**. Some cells have clear cytoplasmic vacuoles. The nuclei have stippled chromatin with single nucleoli and are centralized in the cell. Roughly 1 mitotic figure per 40X field is seen. Multiple sections of the neoplasm fail to show invasion into surrounding soft tissue. Original tumor sections were subdivided to prepare conference slides.

Contributor's Morphologic Diagnosis:
Mammary Gland: ductular carcinoma in situ (DCIS)

Contributor's Comment: Mammary gland tumors are uncommon in macaques. It is still unclear whether the low cancer rate observed in macaques is true resistance or if insufficient lifespan studies have been conducted to see whether higher cancer rates occur in aged populations.[8] Ductular carcinoma in situ (DCIS) are neoplasms that have neoplastic cells limited to ducts. This is distinguished from lobular carcinoma in situ (LCIS) where cells extend into lobules. Occasionally it is difficult to morphologically distinguish LCIS from ductular carcinoma in situ DCIS. A potential marker to distinguish DCIS from LCIS is E-cadherin since E-cadherin protein expression is lost in LCIS, while it remains in cases of DCIS.[6,8] Differentiation between DCIS and LCIS is crucial in humans because management strategies differ greatly between the two types.[7] In humans, estrogens have been hypothesized as contributing to the formation

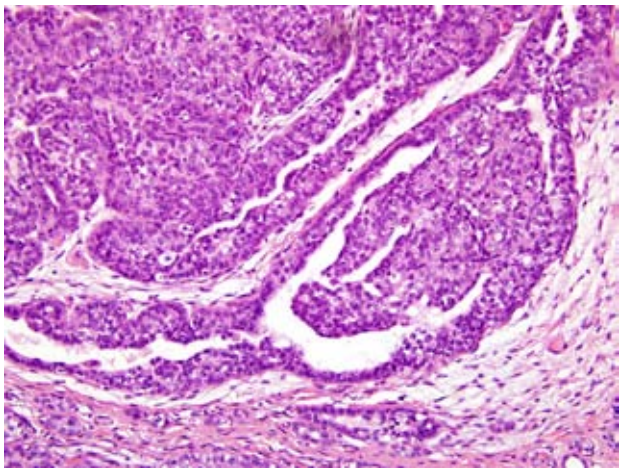

2-1. Mammary gland, macaque. Multifocally, neoplastic cells form micropapillary projections that variably fill duct lumina. (HE 400X).

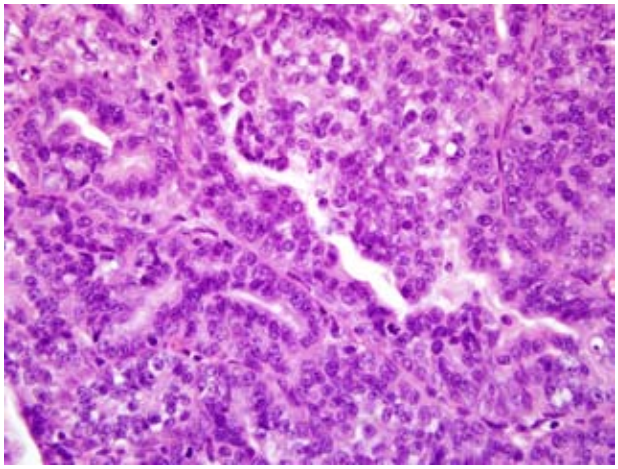

2-2. Mammary gland, macaque. The neoplasm is composed of polygonal to cuboidal cells with variably distinct cell borders, moderate amounts of eosinophilic cytoplasm, round to oval nuclei with finely stippled chromatin and generally 1-3 nucleoli. The mitotic rate is regionally variable with up to 4-5 mitoses in some high powered field. (HE 400X).

of mammary tumors. Estrogen stimulates the mitosis of breast epithelial cells regardless of the gender and can enhance unregulated growth of mammary tissue.[1] This particular case is interesting because it represents a mammary gland carcinoma in a male, which has been rarely reported. One report gives an incidence rate of 1.1% in a long term study of untreated animals.[8] This rate is similar to that seen in men, accounting for 0.8% of all the cases of mammary carcinoma. Most mammary carcinoma in human males is ductal in origin with the majority being invasive. Mammary gland carcinoma in men has been reported to be linked to testicular abnormalities, Klinefelter syndrome, familial history of breast cancer, infertility and breast discharge. They tend to be estrogen and progesterone receptor positive.[3]

AFIP Diagnosis: Mammary gland: Ductular carcinoma in-situ

Conference Comment: This case was reviewed in consultation with the AFIP Department of Gynecologic and Breast Pathology, who agreed with the contributor's diagnosis, and further commented that the DCIS appeared to involve a papilloma, based on the presence of papillary cores within the lesion which are lined by a monotonous proliferation of epithelial cells consistent with DCIS. They also noted the focal presence of myoepithelial cells in some of the papillary cores.

During the post conference, part of the discussion focused on general features distinguishing benign from malignant tumors. These features include pleomorphism, nuclear morphology, appearance of mitotic figures and overall mitotic rate, polarity, and invasiveness.

In malignant tumors, both cells and nuclei generally display greater variation in size and shape than do their benign counterparts. Cells can be much larger or smaller than adjacent cells, with similar variation in nuclear size. These changes are referred to as anisocytosis and anisokaryosis, respectively. In malignant tumors, nuclei often contain an abundance of DNA and stain much darker (hyperchromatic). The nuclear to cytoplasmic ratio can also approach a 1:1 ratio from the normal 1:4 to 1:6 ratio. Mitotic figures are more abundant in malignant tumors than in benign tumors. Often, malignant tumors also have "bizarre mitotic figures" forming abnormal shapes and patterns that do not resemble the normal mitotic rearrangement of chromosomes. These cells often produce multipolar spindles, which can create a highly unusual cellular appearance in relation to neighboring cells. Malignant tumors are generally faster growing neoplasms with growth occurring in a more disorganized, haphazard fashion (often referred to as loss of polarity). Malignant tumors also tend to invade surrounding tissue and metastasize to regional lymph nodes and other organ systems, whereas benign tumors stay in the location of origin. There can be a wide range of morphologic appearances within tumors depending on the specific type of tumor and the tissue involved, so these guidelines are meant as a general rule and are subject to vary from one type of neoplasm to the next.[4]

Mammary gland lesions have been reported in numerous lab animals and domestic species, and a few of the more common of these were discussed during the post-conference session. A chart listing the species discussed during this session and the changes in each species is included below. [2,5]

Species	Mammary change	Cause
Rat	Fibroadenoma (S-D strain)	Increase in prolactin
Rabbit	Mammary dysplasia	Pituitary tumor
Mouse	FVB/N mice – hyperplasia of mammary glands	Proliferation of prolactin secreting cells in pars distalis
	Mammary tumors	Mammary tumor viruses (MMTVs)
Cat	Fibroepithelial hyperplasia	Progesterone administration (Ovaban other iatrogenic hormones)
Canine	Gynecomastia	Sertoli cell tumor

Contributing Institution: National Institutes of Health, Division of Veterinary Resources, Bethesda, MD 20892-5280

References:

1. Clemons M, Goss P: Estrogen and the risk of breast cancer. N Engl J Med **344**:276-285, 2001
2. Foster RA, Ladd PW: Male genital system. *In:* Jubb, Kennedy and Palmer's Pathology of Domestic Animals, ed. Maxie MG, 5th ed., pp. 596-597. Elsevier, Philadelphia, Pennsylvania, 2007
3. Giordano SH, Buzdar AU, Hortobagyi GN: Breast cancer in men. Annals of Internal Medicine 137:678-687. Primatology 2001; 30:121–126
4. Kumar V, Abbas AK, Fausto N: Neoplasia. *In:* Robins and Cotran Pathologic Basis of Disease, ed. Kumar V, Abbas AK, Fausto N, 7th ed., pp. 272-276. Elsevier, Philadelphia, Pennsylvania, 2005
5. Percy DH, Barthold SW: Pathology of Laboratory Rodents and Rabbits, 3rd ed., pp.116-117, 170-171, 306. Blackwell Publishing, Ames, Iowa, 2007
6. Moll R, Mitze M, Frixen UH: Differential loss of E-cadherin expression in infiltrating ductal and lobular breast carcinomas. Am J Pathol **143**:1731–42, 1993
7. Schnitt SJ, Morrow M: Lobular carcinoma in situ: current concepts and controversies. Semin Diagn Pathol **16**:209–23, 1999
8. Wood CE, Usborne A, Tarara R, Starost MF: Hyperplastic and neoplastic lesions of the mammary gland in macaques. Vet Pathol **43**:471–483, 2006

III – Case 36005-7 (AFIP 3094514)

Signalment: Adult male strain MDX mouse; *Mus musculis*; murine

History: The animal is submitted for necropsy for evaluation of a mass involving the right hind limb.

Gross Pathology: The right hind limb contains a large, firm, 2.7 cm x 2.5 cm x 2 cm, pale tan, multilobulated mass extending from the proximal hind limb to the right lateral aspect of the vertebral column. The mass involves the dorsoproximal femur and right lateral lumbar spine, and penetrates into the peritoneal cavity. No other significant gross lesions are observed.

Laboratory Results: N/A

Histopathologic Description: The skeletal and connective tissues of the proximal hind limb surrounding the femur and paralumbar region are effaced by a multinodular, highly infiltrative, and poorly demarcated neoplasm. Confluent nodules are composed of haphazardly arranged, densely cellular, interlacing bundles and streams of plump spindloid to polygonal neoplastic cells. Neoplastic cells exhibit small to moderate amounts of eosinophilic cytoplasm with variably distinct cell borders. Nuclei are large and round to oval or irregularly shaped with coarsely granular to vesicular chromatin and one to three nucleoli. There is marked anisocytosis and anisokaryosis and mitotic figures are numerous (up to eight per 40x field). Present throughout the mass are numerous multinucleated giant cells. Multinucleated cells are distributed throughout the mass and exhibit clustered nuclei with moderate to marked karyomegaly and irregularly lobular nuclei or linearly oriented row of nuclei. Also present within the mass are strap cells, racquet cells and plump polygonal cells with hypereosinophilic cytoplasm (resembling embryonal myocytes) **(Fig. 3-1)**. In multiple regions, neoplastic cells are separated by narrow bands and interconnecting septae of dense, amorphous, deeply eosinophilic matrix resembling osteoid **(Fig. 3-2)**. There are multifocal expanses of necrosis and hemorrhage within the mass.

Within the margins of the tumor adjacent to the lumbar spinal column are multiple fragments of mature cortical bone, necrotic bone, and woven bone. Focally, in association with bone fragments, are small zones of pale basophilic matrix. Along the peripheral margins of the mass, neoplastic cells envelop individualized and atrophic skeletal muscle fibers.

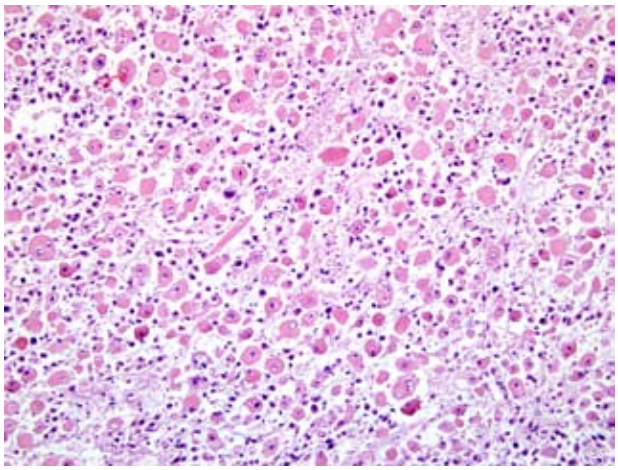

3-1. Muscle, mouse. Within a focally extensive area there are neoplastic embryonal myofibrils characterized by abundant brightly eosinophilic cytoplasm, pleomorphic nuclei with either finely stippled or more coarsely stippled chromatin and separated by a fine fibromyxomatous matrix. (HE 200X).

Immunohistochemistry results for neoplastic cells (Figs. 3-3 and 3-4):

- Vimentin: Diffuse positive cytoplasmic immunoreactivity
- Actin: Multifocal positive cytoplasmic immunoreactivity
- Myogenin: Multifocal positive nuclear immunoreactivity
- Pancytokeratin: Diffusely negative

Contributor's Morphologic Diagnosis: Skeletal muscle: Rhabdomyosarcoma, embryonal

Contributor's Comment: Skeletal muscle neoplasms are rare in both humans and animal species. In humans, rhabdomyosarcoma occurs more frequently than rhabdodmyoma and can be classified into the following categories based on histologic morphology: 1) embryonal rhabdomyosarcoma; 2) botryoid rhabdomyosarcoma; 3) alveolar rhabdomyosarcoma; and 4) pleomorphic rhabdomyosarcoma.[1] Presence of cross-striations in neoplastic cells is variable. Additional histologic types that have been described in humans include anaplastic, monomorphous round cell, spindle cell, lipid-rich/clear cell, and sclerosing rhabdomyosarcoma.[2] Differentiation of subtypes in humans is of prognostic significance, and while rhabdomyosarcomas in animals exhibit similar histomorphologic features, the rarity of these tumors in veterinary medicine hampers evaluation of the prognostic

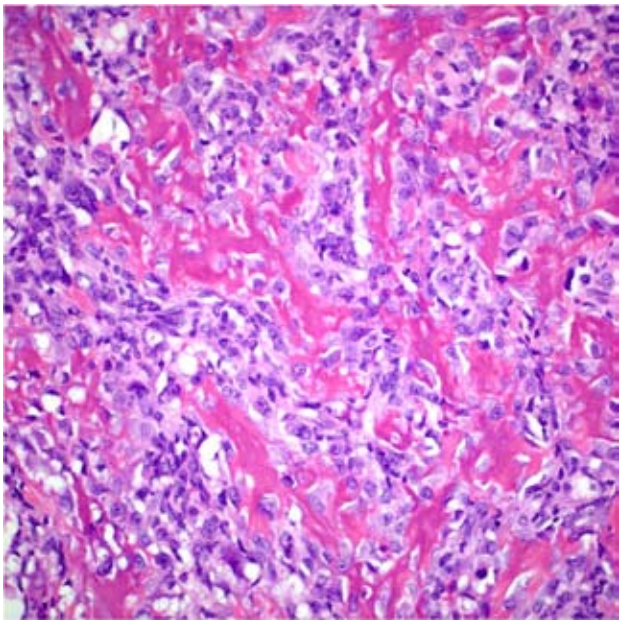

3-2. Muscle, mouse. Neoplastic cells separate and surround osteoid in some areas (HE 400X). Photomicrograph courtesy of Comparative Molecular Pathology unit, Center for Cancer Research, National Cancer Institute Bethesda, MD.

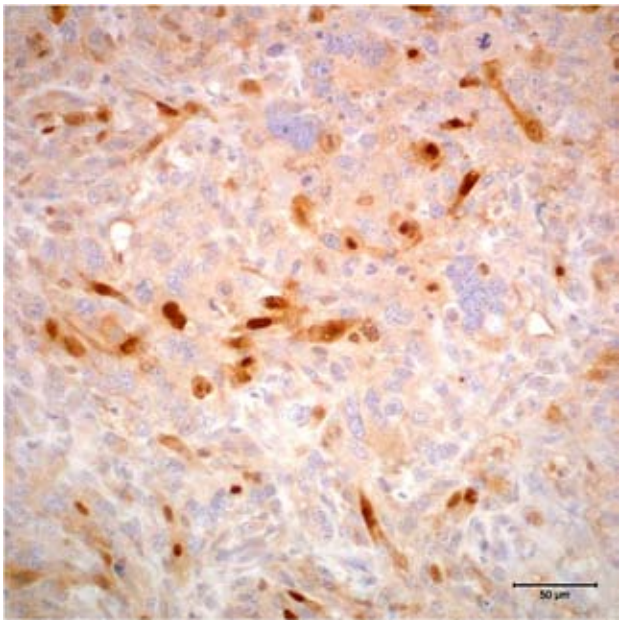

3-3. Muscle, mouse. Multifocal nuclear immuno-positivity for myogenin. Photomicrograph courtesy of Comparative Molecular Pathology unit, Center for Cancer Research, National Cancer Institute Bethesda, MD.

value of such sub-classification.[3]

Most skeletal muscle tumors in animals occur in dogs. Rhabdomyoma and rhabdomyosarcoma have also been reported in cats, cattle, horses, sheep, Sprague-Dawley rats, a Rhesus macaque, and a boa constrictor. In dogs, categorization of rhabdomyosarcomas has included embryonal, botryoid, alveolar, and pleomorphic subtypes, with histologic features of these subtypes in dogs paralleling those described in human cases of rhabdomyosarcoma.[3] The occurrence of laryngeal rhabdomyosarcoma and botryoid rhabdomyosarcoma of the urinary bladder are more commonly described in dogs and may represent distinct clinicopathologic entities in this species.[3]

The degree of expression of immuno-histochemical markers is influenced by the degree of differentiation of neoplastic cells, and staining is often heterogeneous within tumors.[3] Immunohistochemical markers that are described for use in the diagnosis of rhabdomyosarcoma include vimentin, desmin, actin, myoglobin, myosin, titin, myogenin, and myoD1 (myogenic determination factor). More traditionally used immunohistochemical markers, such as vimentin, actin, and myoglobin, are not specific for rhabdomyosarcoma; further, they may not be expressed in more poorly differentiated tumors.[2,11] The

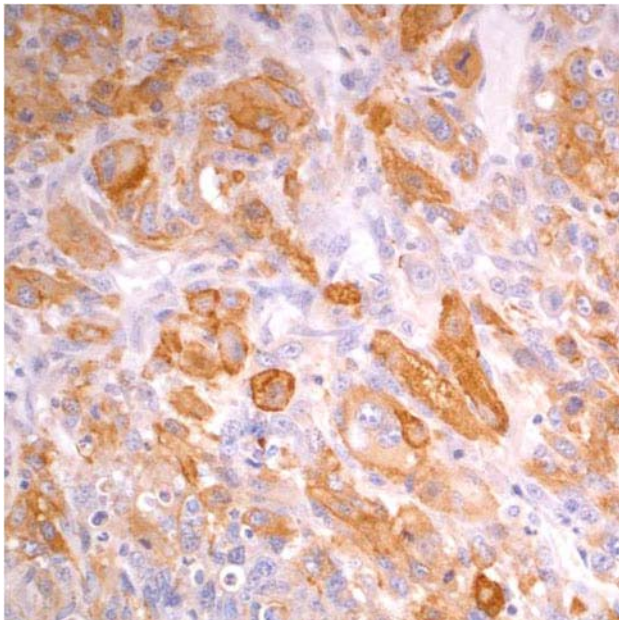

3-4. Muscle, mouse. Multifocal cytoplasmic immunopositivity for actin. Photomicrograph courtesy of Comparative Molecular Pathology unit, Center for Cancer Research, National Cancer Institute Bethesda, MD.

use of transcriptional factors, specifically myogenin and myoD1, for diagnosis of rhabdomyosarcoma has been shown to demonstrate a greater degree of specificity and sensitivity in human tumors.[2,11] Myogenin and myoD1 are preferentially expressed in the nucleus of differentiating myoblasts and are expressed earlier than desmin, muscle-specific actin, myoglobin, and myosin during skeletal muscle development and differentiation.[2,6]

Immunohistochemical analysis for myogenin expression has previously been applied in a mouse model for methylcholanthrene-induced rhabdomyosarcoma. In this model, both embryonal and pleomorphic rhabdomyosarcomas were induced.[6] Immunohistochemistry for myogenin demonstrated expression of myogenin in both pleomorphic and embryonal variants; embryonal rhabdomyosarcomas exhibited greater myogenin expression than pleomorphic types, and myogenin expression was greatest in neoplastic cells of myoblast-like morphology.[6]

Expression of myogenin and myoD1 in two canine botryoid rhabdomyosarcomas was recently evaluated.[6] In these studies, myogenin and myoD1 expression were found to be useful markers for rhabdomyosarcoma in the dog; histomorphology correlated to labeling for myogenin and myoD1. Specifically, myogenin was predominantly expressed by multinucleated cells that expressed alpha-sarcomeric actin, resembling myotubes, while myoD1 was expressed by undifferentiated mesenchymal cells.[8]

The case presented herein exhibits histo-morphologic features that are most compatible with embryonal rhabdomyosarcoma; however, some regions of the tumor are more suggestive of pleomorphic or alveolar variants, including the presence of numerous large multinucleated neoplastic cells and bundles of spindle cells. Strong and widespread positive immunohistochemical reactivity for vimentin, actin, and myogenin support the diagnosis of rhabdomyosarcoma. The majority of neoplastic cells exhibit strong cytoplasmic immunoreactivity for vimentin and actin. Cells expressing nuclear immunoreactivity for myogenin were frequently small and spindloid; myogenin expression was variably present in multinucleated neoplastic cells.

Interestingly, within the neoplastic mass and distal to the site of pathologic fracture are areas of amorphous eosinophilic matrix resembling osteoid. To our knowledge, osteoid formation within a rhabdomyosarcoma has not previously been described. The origin of this apparent osteoid matrix in this neoplasm is uncertain. No cells within the matrix exhibited immunoreactivity for actin or myogenin, which is in contrast to the majority of the neoplastic population.

Signaling morphogenetic proteins via bone has been implemented in the formation of bone by mesenchymal tissues.[4,10] Bone morphogenetic proteins (BMPs) are cytokines within the transforming growth factor-β (TGF-β) family, and signaling occurs via binding to BMP receptors.[10] While BMP expression has been documented to a variable degree in a number of sarcomas, rhabdomyosarcoma was among a subset of tumors that consistently did not show BMP expression as demonstrated by immunohistochemistry.[15]

The focal zone of osteoid formation may represent a response to bone fracture. Bone formation in muscle, referred to as myositis ossificans or myositis ossificans traumatica, is an infrequent sequelae to bone fracture or muscular trauma with hematoma formation.[1,9] Three types of myositis ossificans traumatica are described; two of these types involve the formation of new bone immediately adjacent to or connected to pre-existing bone. The third type of bone formation occurs within a region of muscle that appears to be separate from underlying bone. Theories for the pathogenesis of this type of bone formation have included escape and proliferation of periosteal osteoblasts, metaplasia of intramuscular connective tissue, or induction of osteogenic precursor cells through BMP signaling.[1] The areas of apparent osteoid formation observed in this rhabdomyosarcoma appear at some distance from the site of bone fracture and thus may be most similar to the third type of myositis ossificans traumatica.

AFIP Diagnosis: Skeletal muscle, hind limb: Rhabdomyosarcoma, embryonal with focal osteosarcomatous differentiation

Conference Comments: Conference participants noted a few areas within this neoplasm of osteoid production by neoplastic cells. The ensuing discussion then centered on whether these foci represent tumor bone, areas of osseous metaplasia, or reactive bone secondary to the pathologic fracture of the pelvis or femur. The consensus was that at least in some areas the osteoid was produced by the neoplastic mesenchymal cells. Our diagnosis of rhabdomyosarcoma reflects the predominant line of differentiation (further supported by the contributor's immunohistochemical findings), but also specifies the differentiation towards at least one additional mesenchymal cell type. Some favored the diagnosis of osteosarcoma, arguing that, by definition, if malignant mesenchymal cells are producing osteoid, the tumor is an osteosarcoma, even if other mesenchymal cell types are present.[13] We also considered a diagnosis of malignant mesenchymoma, defined as a malignant tumor consisting of at least two different neoplastic cell lines of

mesenchymal origin.[5,12] In the human literature, it has been suggested to replace the nonspecific designation of 'mesenchymoma' with a classification in one of two ways: by predominant pattern and mention the other, or by the designation as mixed mesenchymal neoplasm and specify the lines of differentiation.[7]

Contributing Institution: Comparative Molecular Pathology Unit, Laboratory of Cancer Biology and Genetics, Center for Cancer Research, National Cancer Institute, National Institutes of Health, 37 Convent Drive, Room 2002, Bethesda, MD 20892

References:

1. Beiner JM, Jokl P: Muscle contusion injury and myositis ossificans traumatica. Clin Orthop Relat Res **403S**:S110-S119, 2002
2. Cessna MH, Zhou J, Perkins SL, Tripp SR, Layfield L, Daines C, Coffin CM: Are myogenin and myoD1 expression specific for rhabdomyosarcoma? Am J Surg Pathol **25**:1150-1157, 2001
3. Cooper BJ, Valentine BA: Tumors of muscle. *In:* Tumors in Domestic Animals, ed. Meuten DJ, pp. 343-357. Iowa State Press, Ames, Iowa, 2002
4. Guo W, Gorlick R, Ladanyi M, Meyers PA, Huvos AG, Bertino JR, Healey JH: Expression of bone morphogenetic proteins and receptors in sarcomas. Clin Orthop **365**:175-183, 1999
5. Hendrick MJ, Mahaffey EA, Moore FM, Vos JH, Walder EJ: Histologic Classification of Mesenchymal Tumors of Skin and Soft Tissues of Domestic Animals, 2nd series, vol. 2, pp. 32-33. Armed Forces Institute of Pathology, Washington, DC, 1998
6. Inoue M, Wu H: mmunohistochemical detection of myogenin and p21 in mehtycholanthrene-induced mouse rhabdomyosarcoma. Int J Exp Path [87]:445-450, 2006
7. Kempson RL, Fletcher CDM, Evans HL, Hendrickson MR, Sibley RK: Atlas of Tumor Pathology, Tumors of the Soft Tissues, 3rd series, fascile 30, pp. 5. Armed Forces Institute of Pathology, Washington, DC, 1998
8. Kobayashi M, Sakai H, Hirata A, Yonemaru K, Yanai T, Watanabe K, Yamazoe K, Kudo T, Masegi T: Expression of myogenic regulating factors, myogenin and myoD, in two canine botryoid rhabdomyosarcomas. Vet Pathol **41(3)**:275-277, 2004
9. Kumar V, Abbas A, Fausto N: Cellular adaptations, cell injury, and cell death. *In:* Robbins and Kotran Pathologic Basis of Disease, ed. Kumar V, Abbas A, Fausto N, 7th ed. p. 11, Elsevier, Philadelphia, PA 2005
10. Nakamura Y, Wakitani S, Saito N, Takaoka K: Expression profiles of BMP-related molecules induced by BMP-2 or -4 in muscle-derived primary culture cells. J Bone Miner Metab **23**:426-434, 2005
11. Parham DM, Ellison DA: Rhabdomyosarcoma in adults and children. Arch Path Lab Med **130**:1454-1465, 2006
12. Pool RR, Thompson KG: Tumors of joints. *In:* Tumors in Domestic Animals, ed. Meuten DJ, 4th ed., pp. 241. Blackwell Publishing, Ames, IA, 2002
13. Thompson KG, Pool RR: Tumors of bone. *In:* Tumors in Domestic Animals, ed. Meuten DJ, 4th ed., pp. 263. Blackwell Publishing, Ames, IA, 2002
14. Vleet JFV, Valentine BA: Muscle and tendon. *In:* Pathology of Domestic Animals, ed. Maxie MG, 5th ed., pp. 272-277. Elsevier Saunders, Philadelphia, PA, 2007
15. Yoshikawa H, Rettig WJ, Lane JM, Takaoka K, Alderman E, Rup B, Rosen V, Healey JH, Juvos AG, Garin-Chesa P: Immunohistochemical detection of bone morphogenetic proteins in bone and soft-tissue sarcomas. Cancer **74(3)**:842-847, 1994

IV – Case 0566-1C (AFIP 3105526)

Signalment: Four mice: 3-month-old, female MyD88-/- *mus musculus* B6/JMyD88N11F4 (*Mus musculus*)

History: The mice are in a full-service room, group housed, on a ventilated rack. Four mice were found with torticollis. The mice were bright, alert, responsive and in good body condition. The laboratory requested a necropsy with culture and sensitivity of the tympanic bullae. Rule outs for head tilt in mice include otitis media/interna, central nervous system disease, and necrotizing arteritis of undetermined cause.

The laboratory has had a number of mice with head tilts in the past and is interested in determining the cause in order to treat or prevent further outbreaks of disease. This is an immune-compromised line that currently is not on antibiotic prophylaxis.

Gross Pathology:

Mice 1 – 3:	Head tilt to the left
Mouse 4:	Head tilt to the right
Mice 1 – 4:	White opaque material within the tympanic bullae
Mice 1, 2, 4:	Swollen right forepaw (up to 0.6 CM in maximum dimension)
Mouse 3:	Not foot lesions

Microbiology:

Mice 1 – 4:	Nasal pharynx culture
Mice 1 – 3:	Tympanic bulla culture
Mice 1, 2, 4:	Forepaw cultured

Laboratory Results: Microbiology Results: Initial

Mouse	Site	Micro #	Bacteria	AMPIC	CEPHA	CHLOR	CIPRO	ERYTH	GENTA	LINCO	PENIC	SXT
1	Foot	M0717948	S. aureus	R		S			S	S	R	S
2	Foot	M0717949	S. aureus	R		S			S	S	R	S
4	Foot	M0717950	S. aureus	R		S			S	S	R	S
			P. mirablis	S		S			S	R	S	S
4	Foot	M0717951	S. aureus	R	R	S			S	S	R	S
1-4	NPX	M0717952	P. mirablis	Proteus mirabilis predominate in all the specimens from the Middle Ear, and 3 of 4 of the Nasal wash had it.								
1-3	Tympanic Bullae											

Complete Antibiotic Culture and Sensitivity Profile: S = Susceptible; R = Resistant

Antimicrobial	Staph. aureus	Proteus mirablis
Amox/Clav AML	S	S
Ampicillin	R	S
Amikacin	S	S
Cefazolin	S	R
Ceftiofur	S	S
Cephalothin	S	S
Chloramphenicol	S	S
Ceftriaxone	S	S
Clindamycin	S	R
Doxycycline	S	R
Enrofloxacin	S	S
Gentamicin	S	S
Norfloxacin	S	S
Penicillin	R	S
Trimethroprim, Sulfamethoxazole	S	S

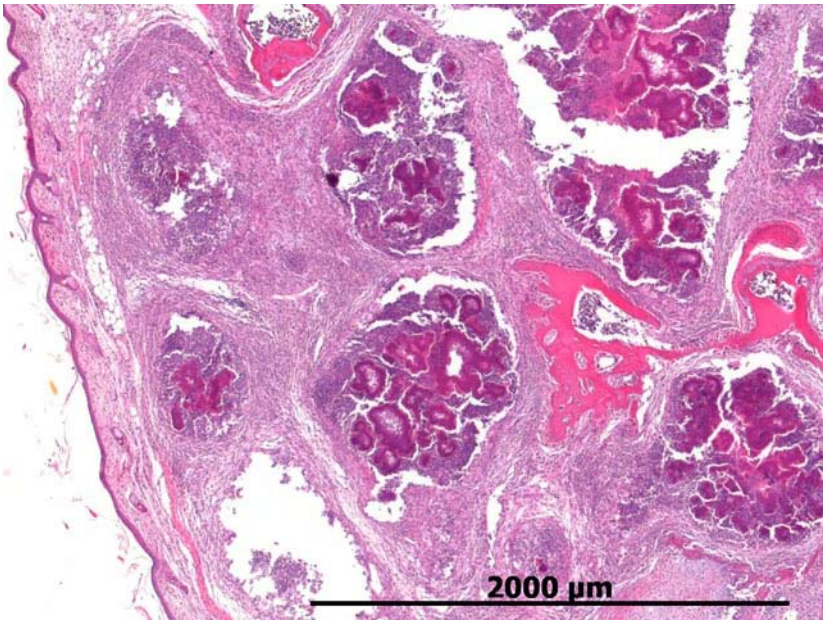

4-1. Forepaw, mouse. Multifocal to coalescing pyogranulomas centered on bacterial colonies surrounded by brightly eosinophilic material. Photomicrograph courtesy of Section of Comparative Medicine, School of Medicine, Yale University New Haven, CT.

Histopathologic Description: The forepaw is markedly expanded by numerous coalescing botryoid pyogranulomas centered on 100-200 um colonies of Gram-positive cocci, surrounded by brightly eosinophilic amorphous material (Splendore-Hoeppli) **(Figs. 4-1 and 4-2)**. These pyogranulomas contain a central core of abundant necrotic debris admixed with numerous neutrophils, surrounded by layers of epithelioid macrophages, fewer lymphocytes and plasma cells, and finally, outer layers of fibroblasts and collagen. In the adjacent tissue there is marked thinning and loss of bone of the distal phalanges. In addition, there is edema with macrophages, lymphocytes, and plasma cells within the subcutaneous tissue.

Contributor's Morphologic Diagnosis: Cellulitis, pyogranulomatous and necrotizing, focally extensive, subacute, severe with Splendore-Hoeppli material and large colonies of cocci

Contributor's Comment: Myeloid differentiation factor 88 (MyD88) knockout mice have been shown to be deficient in the production of an innate immune response.[7,8,12] Neutrophil function is compromised due to the deletion of MyD88 from the signaling pathway of toll-like receptors (TLR). The immune response has also been shown to be delayed due to failure of proinflammatory cytokines and induction of NF-kB and MAP-kinase pathways.[1,2,12] Impairment of macrophage function, especially in the production of IL-6 and TNF-a, has been shown in response to LPS, peptidoglycan, and lipopeptides.[7,14] The model has also been shown deficient in the response to exogenous IL-1 as the production of TNF-a and IL-6 is muted.[13] The failure of a normal macrophage response also resulted in a decreased B cell response. Although the initial response to LPS in diminished, the overall deleterious effects to the animal are increased as sepsis results in hyperinflammation.[12] The decreased immune response of MyD88 knockout mice has been described in a variety of tissues, including brain [7], skin [10], and generalized infections.[12]

Reported causative agents of botryomycosis include *Staphylococcus aureus, S. hominus, S. xylosus, Pseudomonas aeruginosa, Proteus* spp.*, Escherichia coli, Nocardia asteroides* and *Streptococcus intermedius*, with a variety of other aerobic and anaerobic bacterial agents implicated.[3,9,11,14,15] Immunosuppression has been suggested as a factor in increased prevalence of botryomycosis.[11,16] As described above, the MyD88 knockout mouse is deficient in the innate immune response.

Splendore-Hoeppli staining refers to the deeply eosinophilic material that surrounds the 'grains' of bacterial colonies contained centrally. The eosinophilic material is described as having a coronal appearance, which engulfs whitish purulent material associated with the colonies[3,14,15]. Necrotic tissue has also been reported to be present.[3] While Splendore-Hoeppli bodies are predominately reported to be associated with botryomycosis, numerous reports of this phenomenon in the presence of parasitic [3] or fungal infections [4,15,16] are in the literature. The eosinophilic staining component of this histologic finding has been linked to cellular debris and antigen-antibody complexes.[3,11,15] This staining

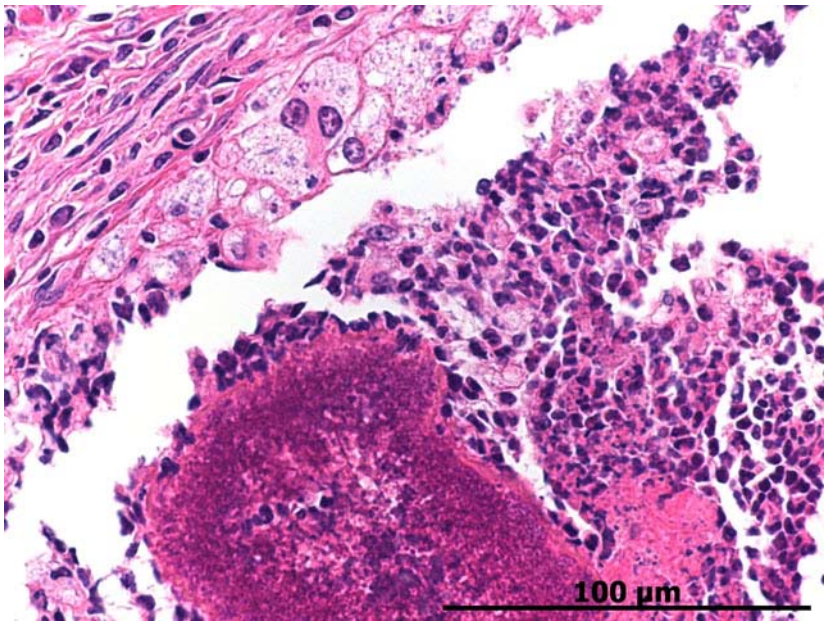

4-2. Forepaw, mouse. The pyogranulomas are centered on bacterial colonies composed of 1-2 micron diameter cocci that are surrounded by a radiating corona of brightly eosinophilic club shaped material (Splendore-Hoeppli material) admixed with necrotic debris, neutrophils and bounded by epithelioid macrophages, lymphocytes, fibroblasts and fibrous connective tissue. Photomicrograph courtesy of Section of Comparative Medicine, School of Medicine, Yale University New Haven, CT.

pattern has been referred to as Splendore-Hoeppli bodies, material, and phenomenon.

The lesions in the forepaw were subsequently determined to be secondary to toe-clip for identification. The colony was subsequently placed on Baytril and there were no further lesions.

AFIP Diagnosis: Digits, foreleg: Cellulitis, pyogranulomatous and necrotizing, subacute, focally extensive, severe with osteolysis, Splendore-Hoeppli material and large colonies of cocci

Conference Comment: Botryomycosis, a disease of the skin and subcutis, is caused by nonfilamentous bacteria that form grossly visible colonies that look like granules or spicules within a chronically affected lesion. This condition generally affects the skin, but it can extend into deeper tissues if left untreated. Rule outs for these lesions include actinomycotic and eumycotic mycetomas. Infections generally start after trauma to the skin or wound contamination.[6]

Botryomycosis usually manifests as a firm nodule that is ulcerated with a draining tract. The discharge often contains the previously described granules or spicules, thus suggesting botryomycosis. Histologically, this is a striking lesion with a marked pyogranulomatous response centered on bacterial colonies often encircled by Splendore-Hoeppli material. These lesions can be walled off by abundant fibrous connective tissue and can coalesce to form chains of granulomas within the subcutis and surrounding tissues.[6]

Contributing Institution: Section of Comparative Medicine, School of Medicine, Yale University New Haven, CT http://info.med.yale.edu/compmed/compmed/index.htm

References:

1. Akira S and Takeda K: Toll-like receptor signaling. Nature Reviews **4**:499-511, 2004
2. Akira S: Toll-like receptors: lessons from knockout mice. Biochem Soc Trans **28**:Part 5, 2000
3. Armed Forces Institute of Pathology: Wednesday Slide Conference, Conference 13, Case 1, AFIP #2812387, Conference Comments, 2006
4. Bersoff-Matcha Sj, Roper CC, Liapis H, and Little JR: Primary Pulmonary Botryomycosis: Case Report and Review. Clin Infec Dis **26**:620–624, 1998
5. EL van den Berk G, Noorduyn LA, van Ketel RJ, van Leeuwen J, Bemelman WA, and Prins JM: A fatal pseudo-tumour: disseminated basidiobolomycosis. BMC Infectious Diseases **6**:140, 2006
6. Ginn PE, Mansell JEKL, Rakich PM: Skin and appendages. *In:* Jubb, Kennedy and Palmer's Pathology of Domestic Animals, ed. Maxie MG, 5th ed., pp. 691. Elsevier, Philadelphia, Pennsylvania, 2007
7. Goldstein DR, Tesar BM, Akira S, and Lakkis FG: Critical role of the Toll-like receptor signal adaptor protein MyD88 in acute allograft rejection. J Clin Invest **111(10)**: 1571-1578, 2003
8. Kielian T, Phulwani NK, Esen N, Syed MM, Haney AC, McCastlain K, and Johnson J: MyD88-dependent signals are essential for the host immune response in experimental brain abscess. J Immunol **178**:4528–4537, 2007

9. Machado CR, Schubach AO, Conceição-Silva F, Quintella LP, Lourenço MCS, Carregal E, and do Valle ACF: Images in Clinical Dermatology. Dermatology **211**:303-304, 2005
10. Rodig SJ and Dorfman DM: Splendore-Hoeppli phenomenon. Arch Pathol Lab Med **125**:1515-1516, 2001
11. Schlossberg D, Pandey M, and Reddy R: The Splendore-Hoeppli phenomenon in hepatic botryomycosis. J Clin Pathol **51**:399-400, 1998
12. Sugawara I, Yamada H, Mizuno S, Takeda K, and Akira S: Mycobacterial infection in MyD88-deficient mice. Microbiol Immunol **47(11)**:841-847, 2003
13. Tohno M, Skimazu T, Aso H, Kawai Y, Saito T, and Kitazawa H. Molecular Cloning and Functional Characterization of Porcine MyD88 Essential for TLR Signaling. Cell Mol Immunol **4(5)**:369-376, 2007
14. Weighardt H, Kaiser-Moore S, Vabulas RM, Kirschning CJ, Wagner H, and Holzmann B: Cutting edge: Myeloid differentiation factor 88 deficiency improves resistance against sepsis caused by polymicrobial infection. J Immnunol **169**:2823–2827, 2002
15. Zaharopoulos P: Fine-needle aspiration cytologic diagnosis of lymphocutaneous sporotrichosis: A case report. Diag Cytopathol **20(2)**:74-77, 1998
16. Zavasky D, Samowitz W, Loftus T, Segal H, and Carroll K: Gastrointestinal zygomycotic infection caused by basidiobolus ranarum: Case report and review. Clin Infec Dis **28(6)**:1244-8, 1999